JCTC Journal of Chemical Theory and Computation

On the Balance of Simplification and Reality in Molecular Modeling of the Electron Density

Peter L. Warburton,*,† Jenna L. Wang,‡ and Paul G. Mezey†,§

Scientific Modeling and Simulation Laboratory (SMSL), Department of Chemistry and Department of Physics and Physical Oceanography, Memorial University of Newfoundland, St. John's, Newfoundland A1B 3X7, Canada, Molecular Graphics and Modeling Laboratory, University of Kansas, Lawrence, Kansas 66045, and Institute for Advanced Study, Collegium Budapest, Szentháromság utca 2, 1014 Budapest, Hungary

Received July 9, 2008

Abstract: Fused-sphere (van der Waals) surfaces and their variants such as solvent accessible surfaces and molecular surfaces are simple molecular models that are commonly used for many diverse purposes across a broad range of scientific disciplines due to their low computational resource demands. Fused-sphere models require atomic radii to be defined. Many different atomic radii have been proposed, with each set of radii being applicable to a relatively limited scope of molecular types or situations. The large number of differing radii sets actually serves to emphasize the simplicity of the model and its inability to accurately represent the reality of the molecule: its electron density. By measuring the similarity of fused-sphere, fuzzy fused-sphere, and calculated electron density representations of a set of small molecules via symmetric volume differences and the shape group method, it can be seen that fused-sphere models are very poor at representing the real electronic charge distribution of small molecules, especially where π bond systems, lone pair electrons, and aromatic rings are involved. Larger molecules, conceivably, will be even more poorly represented. With advances in computational power and modeling techniques to arrive at high-quality calculated electron density representations for large molecules already in existence, abandoning the use of fused-sphere models should be considered for many applications.

Introduction

Fused-sphere surfaces based upon the addition of rigid spherical representations of atoms defined by their van der Waals radii[1] are commonly used as simple models of molecular systems. Derivative models based on van der Waals surfaces,[2] where a spherical solvent molecule of a certain radius is rolled over the van der Waals representation, include the solvent-accessible surface and the molecular surface (solvent-excluded surface). In the solvent-accessible surface, the derivative surface is the envelope of points the center of the solvent molecule occupies as it is rolled over the van der Waals surface, while the molecular surface is the envelope of points of closest approach between the van der Waals surface and the solvent sphere surface as it is rolled along the original surface.

Applications using these fused-sphere models can fall into several categories. In one category property values such as lipophilicity[3] or electrostatic potential[4,5] are determined at points on the surface to help in defining force field[5−7] and solvation[4,7−11] models which are used to describe phenomenon ranging from molecular docking,[3] to molecular mechanics,[5−7] to calculated energetics,[8] to solute−solvent nuclear Overhauser effects.[9] In another category, fused-sphere models are used to determine molecular surface areas

* Corresponding author phone: (709)737-6939; fax: (709)737-3702; e-mail: peterw@mun.ca. Corresponding author address: Department of Chemistry, Memorial University of Newfoundland, St. John's, Newfoundland A1B 3X7, Canada.

† Memorial University of Newfoundland.

‡ University of Kansas.

§ Collegium Budapest.

10.1021/ct800268c CCC: $40.75
Published on Web 09/10/2008

and volumes[2,12−25] which are then used to investigate many properties of proteins from folding[12] and packing density[13,14] to docking[15] and hydrophobicity[19] as well as molecular solid-state reactivity[16] and molecular connectivity indices for QSAR purposes.[25] In a third category, investigations of weak interactions in molecular systems often rely on the concept that a weak bond between atoms exists if the interatomic distance is shorter than the sum of the van der Waals radii.[26−28]

Determining the van der Waals radius for an atom is not a straightforward process, as the many proposed values of atomic radii[1,12−18,29−37] indicate. Many van der Waals radii values have been obtained from measurements of the nonbonding contact distances between atoms in crystal structures.[1,13−17,29−33] One drawback to this source of radii is that often hydrogen atoms are not clearly seen within the structure, and so they are either ignored, or the radii of the functional group including the hydrogen atoms are defined.[15,33] A second drawback is that a specific atom must either be represented by an average radius value, or by several different radii, depending on the environment it is found in.

Attempts at defining van der Waals radii based on electrostatic principles or SCF calculations[34−39] have also been made. However, these values often differ from each other because they are dependent on an appropriate cutoff condition. Various conditions proposed are cases where the radii in the model system result in appropriate binding[34] or repulsion energies,[35] or on numerical factors based on row constants, number of valence electrons and the Born exponent,[36] or on a fixed electron density value calculated from the ratio of the Dirac exchange constant and the Thomas-Fermi kinetic energy constant.[37] The use of a pseudopotential based calculations to derive adjustable atomic radii, mainly for transition metals, has also been considered,[38] as has the concept of bond valence.[39]

The defining of several different or adjustable radii[12−15,18,33,35,38] for the same atom (or functional group) arises from the concept that the atomic environments can differ due to bonding (e.g., C−H bond versus C−O bond), atom hybridization, or relative atomic position (e.g., the interior versus exterior of a protein). This use of several different radii then serves to reduce the issue of a single representative atomic radius being used to describe all like atoms but only does so to the extent that two or more representative radii are used instead. Also ignored in fused-sphere modeling is the concept of anisotropicity, where the atomic electron distribution is not spherical. This has been shown not only in a calculated electron density study[35] but also in crystallographic studies of specific atomic interactions, such as sulfur−sulfur[40] and chlorine−chlorine.[41] Also, in the case of weak bonding interactions it has been stated that the use of the sum of van der Waals radii as an indicator of interaction should be discarded, mainly due to the lack of precision in van der Waals radii, especially for metals.[42]

Derivative fused-sphere surfaces such as the solvent-accessible and solvent-excluded surfaces are sometimes seen to resolve another issue of fused-sphere surfaces, where the regions of overlap between two spheres do not provide a smooth transition from the surface of the first atom to the second, but rather the transition occurs through a nondifferentiable cusp point. This is more similar to what happens in real electron densities, which by their fuzzy natures have smooth transitions between atoms in bonding and overlap regions. However, the derivative fused-sphere models accomplish this not by modeling the molecule itself but rather a specific molecule-solvent interaction that will change with a change in solvent sphere choice. It has also been suggested that particular regions of the modeled molecule will interact differently with a chosen solvent than will other regions, and so variable solvent sphere radii need to be used in relation to a single molecule to give a more reasonable derivative fused-sphere model.[18]

Alternative simple models have been proposed to replace fused-sphere models. Most of these alternatives involve the addition of Gaussian-based functions instead of hard fused-spheres to model the atoms.[3,43−47] The reasons for proposing these models center on "scientific accuracy"[43] or convenience,[44] as Gaussian based functions are easily integrated or differentiated, and the products of Gaussians have useful coalescence properties.[45] As the addition of Gaussian functions does not lead to cusp regions in between atoms, such representations often match the solvent-excluded surfaces very well, especially if the Gaussians are chosen to have a radial distribution that matches closely a predetermined set of hard sphere van der Waals radii.

Pacios has also proposed and used a simplified representation of electron densities that could be used as an alternative to hard-sphere models[48−52] that are not based upon Gaussian functions but rather a parametrized radial distribution function arrived at from exponential function descriptions of the core and valence electrons.

While molecular shape-effects may become manifested in a whole variety of ways (for example, in solute−solvent interactions as well as in various statistical treatment of solutions), the evident fact remains: the shape of a molecule is the shape of the actual material making up the molecule-the atomic nuclei and the electronic density cloud. Since there is nothing else there, and the nuclei are buried within the electron density, the shape of a molecule is determined by the electron density cloud at the fuzzy, peripheral regions of molecules. Therefore, the shape of the electron density is the shape of the molecule. Evidently, any aspect of molecular shape must also ultimately depend on the electron density. This follows from the Hohenberg−Kohn theorem,[53] which states that the ground-state electron density fully determines the Hamiltonian and, hence, any other property of the molecule. Therefore, even for shape problems related to molecular interactions, it is natural to deal with electron density, since the very interactions must occur between and ultimately must depend upon the electron densities of the interacting molecules. For any interactions among a finite number of molecules, the molecular assembly can be regarded as a supermolecule, and all statements valid for the electron density shape characterization of individual molecules automatically also apply to the entire assembly, even if technically such computations might become more complex. Nevertheless, the principles are the same: electron density provides the ultimate shape representation.

The holographic electron density theorem provides an even stronger statement of the use of electron density as the means to define molecular shape: for real, boundaryless molecules in the electronic ground state, it has been proven that any positive volume part of the electron density of a molecule must also contain *all* of the information that is contained in the complete electron density of the molecule.[54] As an extension of the Hohenberg−Kohn theorem, this leads to the conclusion that any finite electron density piece (whether defined as a piece from a single molecule compared to the complete electron density of the molecule or defined as the nearly complete electron density of an individual molecule which is treated as a finite piece of the supermolecular electron density which describes a finite set of interacting molecules) must also contain all the information that would be found in complete ground-state electron density that determines all properties of the system.[55]

To show that fused-sphere models (either hard-sphere or Gaussian-based) are inadequate in modeling the fundamental nature of the molecule (its electron density), a set of 46 small molecules was tested. For each molecule, a hard-sphere representation, a Gaussian-based fuzzy fused-sphere representation, and several calculated electron density representations from basis sets of differing size were created. The similarities between these representations was measured by looking at the equivolume symmetric volume differences between the surface representations as well as the shape similarity of the distribution of electron density between the fuzzy fused sphere and the calculated representations. The results of these similarity comparisons show that, at best, hard-sphere models represent well the electron density of sigma-bonding-only molecules as calculated with a minimal basis set. Increases in basis set size, which are associated with a providing a better modeled representation of actual molecular electron density, also increase the differences seen between the calculated electron density representations and the fused-sphere models. A spherical representation of an atom is shown to be inadequate in modeling pi bonding systems and atoms with lone pairs. As small molecules are poorly represented, the inference that larger molecules will be even more poorly represented is a logical one. With advances in parallel computing and linear scaling electron density methods,[56−59] a movement away from fused-sphere models and toward calculated electron density-based models should be considered.

Theory

Two means of measuring the similarity of molecular representative surfaces were used: symmetric volume differences and the shape group method.[60−66] In the symmetric volume difference method the similarity of two equal-volume enclosing surfaces expressed on the same molecular configuration K (G_K and G'_K) is measured by the volume enclosed by the intersection of surfaces G_K and G'_K ($V_{G\cap G'}$) subtracted from either volume V_G or $V_{G'}$. Because the surfaces enclose equal volumes, the measure is symmetric: $V_G - V_{G\cap G'} = V_{G'} - V_{G\cap G'}$. Surface similarity is expressed by volume difference. Two surfaces with a small volume difference are more similar than two surfaces with a greater volume difference. The relative symmetric volume difference can be expressed as the ratio between the symmetric volume difference and the volume enclosed by one of the surfaces. Figure 1 shows a graphical example of the symmetric volume difference method. It should be noted in the figure that a two-dimensional slice of a three-dimensional model is shown. Therefore, while the areas enclosed by the surfaces in the figure may not be equal, over the entire three-dimensional model, the enclosed volumes are equal.

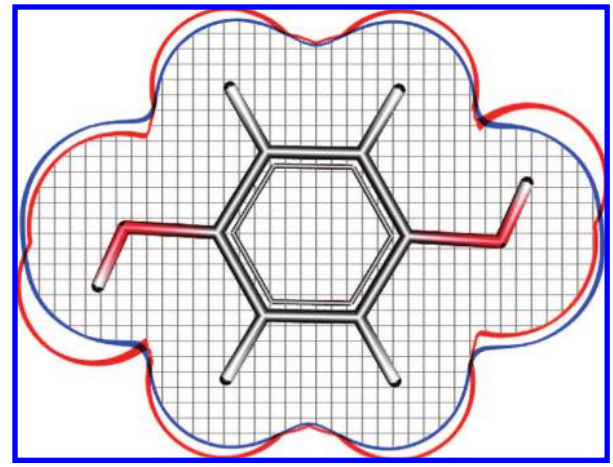

Figure 1. An example of the symmetric volume difference measurement of similarity. The volume enclosed by the intersection of the red and blue surfaces (the patterned region) is subtracted from the volume enclosed by either the red or blue surface. Since the surfaces are chosen to enclose equal volumes, this defined volume difference is the same for either the red or the blue surface.

The shape group method provides consistent description of the shapes of molecules based on electron density representations. These descriptions can be compared to provide a single numerical measure of the similarity of two electron density representations.

Since electron density representations are fuzzy, the shape group method uses molecular isodensity contours (MIDCOs) to allow for the use of discrete mathematics. In three-dimensional space, a MIDCO $G(a)$ based upon molecular configuration K is defined for the fuzzy electron density representation $\rho(\mathbf{r})$ such that each point in the MIDCO has the same electron density value a: $G(a) = [\mathbf{r} \in \mathscr{R}^3: \rho(\mathbf{r}) = a]$, $a \in \mathscr{R}^3$. Because the boundary value a can vary continuously throughout the space, a continuum of MIDCOs exist.

The shape characterization of a given MIDCO is performed based upon the local relative curvature properties of all the points that lie on the MIDCO surface.[66] Mathematically, the local curvature at the surface point of interest can be fully described by defining two orthogonal vectors that form the basis of the plane tangent to the surface point. These two vectors, combined with the electron density gradient vector, define a local coordinate frame for the three-dimensional space with the origin at the surface point of interest. For some specific choice of tangent plane vectors (the eigenvectors), the 2×2 Hessian matrix description of the tangent plane will have the eigenvalues h_1 and h_2 that describe the surface curvature relative to the tangent plane.

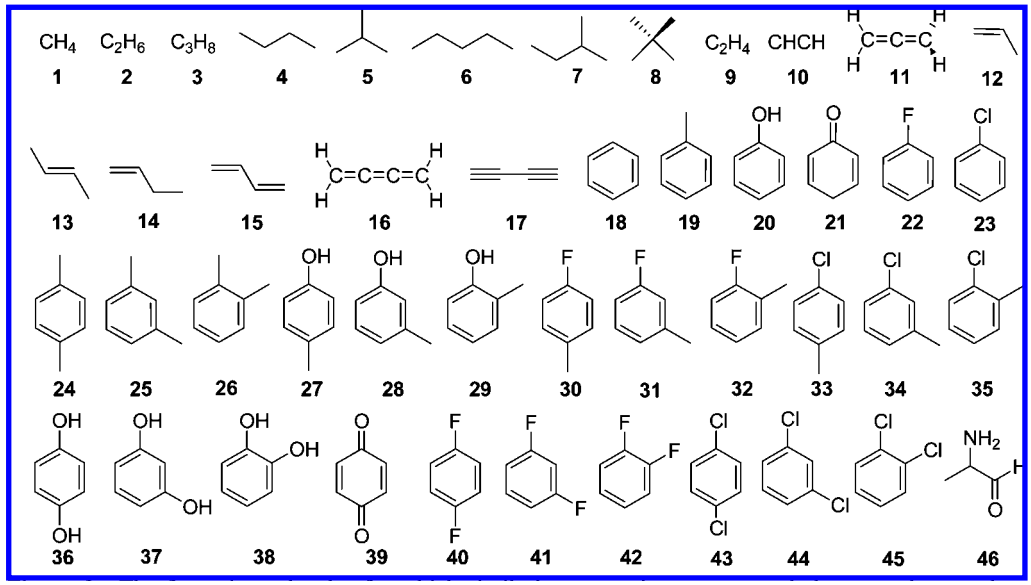

Figure 2. The 46 molecules for which similarity comparisons were made between the van der Waals, fuzzy fused-sphere, and calculated electron density surfaces.

The local relative curvature is measured compared to a reference curvature defined by a parameter b expressed as a sphere with radius $1/|b|$. A positive value of b results in a sphere that curves toward the interior of the surface, a negative value of b curves toward the exterior of the surface, and a zero value for b represents the tangent plane to the point of interest. The local relative curvature is found by a direct comparison of the eigenvalues of the Hessian matrix to the value of b. The surface point is locally convex compared to the reference curvature if $h_1 \leq h_2 < b$ and can be said to belong to domain $D_2(b)$. The point is locally concave and belongs to domain $D_0(b)$ if $b \leq h_1 \leq h_2$. Finally, the point is locally saddle (domain $D_1(b)$) if $h_1 < b \leq h_2$.

When all of the surface points of a MIDCO are assigned to curvature domains, the shape of the MIDCO relative to the reference curvature can be described. If all locally convex points are truncated from the surface, the remaining MIDCO points define one or more distinct surface pieces. Each piece may be closed or have one or more holes. Through the use of homology groups[60] each piece of the truncated surface can be assigned three Betti numbers B_p ($p = 0$, 1, or 2) based upon the incidence of oriented point, line, and area pieces to one another. If $B_0 = B_2$, then by the Poincaré index theorem for a two-dimensional surface the piece is a closed surface and has no holes. If $B_0 \neq B_2$, then the piece is open and is topologically equivalent to a sphere with a hole in it. All such open disconnected pieces in the truncated surface share a common hole, which serves to describe their disconnection from each other. Additional holes may also be present in a piece. The number of such holes is given by the first Betti number B_1. Therefore, the total number of holes for the piece is given by the first Betti number B_1 plus the common hole to all pieces, leading to B_1+1 holes. The shape of the MIDCO is described by the *shape ID vector*, which is the ordered list of B_1+1 values for all the pieces.

Since the ordered lists of the shape ID vectors can be unwieldy to compare, the description of the shape of the MIDCO can be further encoded by defining the *shape ID number* $c'(a,b)$ based upon a prime number encoding scheme of the ID vector. If the shape ID vector is ordered from the largest magnitude Betti number (B1) to the smallest (Bn), then $c'(a,b) = 2^{B1+1} \times 3^{B2+1} \times 5^{B3+1} \times ... \times P_n^{Bn+1}$.

The shape ID numbers are easily compared, but are only valid for comparison between MIDCOs of the same isodensity a and reference curvature b. Since there are infinitely many choices for these variables, different values will result in different shape descriptions of the same molecule. Total shape characterization of a molecule is achieved through a collection of shape codes at various combinations of variable values. In the current implantation of the method, 41 MIDCOs $G(a)$ are chosen throughout the range 10^{-3} e$^-$/bohr$^3 \leq a \leq 10^{-1}$ e$^-$/bohr^3 and are analyzed at 21 reference curvature values (10^{-5} bohr $\leq |b| \leq 1$ bohr and also $b = 0$ bohr). The complete shape of the molecule is described by an 861 (41×21) member *(a,b)-map* matrix of shape codes.

Finally, the measurement of the similarity of electron density representations of molecules is given by the single-valued *shape similarity index* $S(X,Y)$. For molecules X and Y, the *shape equivalence* (Δ) of the molecules at isodensity a and curvature b is one if they have the same shape code, and zero if they do not. The shape similarity index is the sum of the shape equivalence values for all matrix elements of the (a,b)-map divided by the total number of elements.

Computational Approach

For each of the 46 molecules examined (Figure 2), a single geometry optimized at the HF/6−31G** level with *Gaussian03*[67] was used as a basis for all subsequent calculations. van der Waals surfaces were generated on a grid of 0.1 bohr utilizing the atomic radii of Gavezzotti.[16] Use of a grid allowed for direct comparison of the van der Waals surface to the grid-based electron density representations in the study.

Electron density representations were calculated on a 0.1 bohr grid utilizing several different basis sets with the Hartree−Fock methodology using an in-house program and

Table 1. Similarity Comparisons for Sigma-Bonded Molecules **1**-**8**[a]

		STO-3G				3−21G			
	V_{VDW}[b]	CED-VDW[c]	FFS-VDW[c]	FFS-CED[c]	shape[d]	CED-VDW[c]	FFS-VDW[c]	FFS-CED[c]	shape[d]
1	189.6	2.93%	2.46%	1.61%	0.85	3.48%	2.58%	1.81%	0.90
2	294.2	2.63%	2.05%	1.16%	0.91	3.45%	2.63%	1.21%	0.89
3	404.1	2.60%	2.02%	1.08%	0.95	3.40%	2.78%	1.10%	0.86
4	519.1	2.69%	2.11%	1.10%	0.95	3.59%	2.98%	1.21%	0.87
5	514.2	2.67%	2.16%	1.04%	0.94	3.52%	2.96%	1.11%	0.86
6	626.1	2.67%	2.14%	1.02%	0.91	3.55%	3.02%	1.14%	0.85
7	624.2	2.61%	2.14%	0.98%	0.94	3.46%	2.96%	1.05%	0.85
8	624.8	2.85%	2.42%	1.13%	0.92	3.77%	3.17%	1.32%	0.93

		6−31G**				cc-pVDZ			
	V_{VDW}[b]	CED-VDW[c]	FFS-VDW[c]	FFS-CED[c]	shape[d]	CED-VDW[c]	FFS-VDW[c]	FFS-CED[c]	shape[d]
1	189.6	3.16%	2.51%	0.69%	0.87	3.75%	2.97%	1.02%	0.69
2	294.2	2.77%	2.57%	0.84%	0.87	3.43%	3.53%	1.41%	0.62
3	404.1	2.77%	2.75%	0.89%	0.86	3.43%	3.78%	1.47%	0.59
4	519.1	2.89%	2.95%	0.97%	0.89	3.62%	4.06%	1.48%	0.65
5	514.2	2.88%	2.97%	0.84%	0.89	3.57%	3.96%	1.34%	0.61
6	626.1	2.88%	3.01%	1.02%	0.86	3.60%	4.10%	1.55%	0.62
7	624.2	2.82%	2.97%	0.88%	0.86	3.51%	3.95%	1.33%	0.63
8	624.8	3.18%	3.24%	0.88%	0.87	3.81%	4.09%	1.31%	0.66

[a] CED − calculated electron density, FFS − fuzzy fused-sphere, VDW − van der Waals. [b] V_{VDW} − van der Waals surface volume in $bohr^3$/molecule. [c] Symmetric volume difference of the two specified surfaces expressed as a percentage of V_{VDW}. [d] Shape group method similarity between CED and FFS.

the full population analysis performed by *Gaussian03*. Additionally, electron density representations of the individual atoms in their ground states were calculated on a 0.08 bohr grid in the same manner. These atomic representations were then added together in a 0.1 bohr grid to give the fuzzy fused-sphere electron density representations. Use of a higher resolution grid for the atomic fragments served to reduce the error that would be caused by nuclear positions that did not sit exactly on any of the face-centered cubic positions of the grid cells. In all cases, the placement and orientation of the molecule within the grid was defined based on the standard orientation of the *Gaussian03* output, with the origin of the space placed exactly in the center of a grid cell.

The volumes enclosed by the van der Waals surfaces were calculated numerically. Electron density surfaces for both the calculated and fuzzy fused- sphere representations enclosing the same volume as the van der Waals surface were then found through an iterative process of adjusting the isosurface value and numerically calculating the enclosed volume. Because all molecular representations were created in the same grid space, the symmetric volume difference between surfaces was also calculated numerically.

Shape similarity comparisons between fuzzy fused-sphere and calculated electron density representations of molecules were carried out with a suite of in-house programs.

Results and Discussion

The molecules studied were subdivided into groups based upon their bonding. Alkanes **1**-**8** display only sigma bonding, while molecules **9**-**17** and **46** show both pi and sigma bonding. The remaining molecules contain an aromatic ring, with the exception of **21** and **39**, though these molecules are included in the aromatic group because of their ring structure and high degree of conjugation.

Table 1 shows the comparison of the van der Waals (VDW), fuzzy fused-sphere (FFS), and calculated electron density (CED) surfaces for the alkane sigma-bonding group of molecules at four different basis set levels using relative symmetric volume differences. Additionally, the shape group method similarity values between the fuzzy fused-sphere and calculated electron density representations of the molecules are given.

In terms of calculated electron densities, those calculated at the HF/STO-3G level are considered to be the least representative of realistic electron densities, both because the Hartree−Fock method does not account for electron correlation, and because the STO-3G basis set is small. The minimal nature of the basis set does not allow for robust representation of molecular orbitals, to the point where the HF/STO-3G calculated electron density can be thought of as fused-atom representations of the molecules with slight distortions seen in the bonding regions. This notion is borne out in the data of Table 1. The fuzzy fused-sphere representations of the molecules have smaller relative symmetric volume difference values compared to the van der Waals surface (FFS-VDW) than do the calculated electron density representations (CED-VDW), indicating the fuzzy fused-sphere representations are more similar to the van der Waals representations. However, the fuzzy fused-sphere and calculated electron density representations are very similar to each other (FFS-CED) because the addition of fuzzy spheres will better model the off-bond portion of the sigma-bonding regions of the molecules compared to discrete fused-sphere representations. This is not surprising, as a disadvantage of van der Waals surfaces is the poor representation of the electron density in the bonding regions where the spheres overlap. Molecular surface representations counteract this disadvantage somewhat and should end up being more similar to the fuzzy fused-sphere representations than to the

Table 2. Similarity Comparisons for Molecules with Sigma and Pi Bonding[a]

		STO-3G				3−21G			
	V_{VDW}[b]	CED-VDW[c]	FFS-VDW[c]	FFS-CED[c]	shape[d]	CED-VDW[c]	FFS-VDW[c]	FFS-CED[c]	shape[d]
9	263.3	3.59%	4.55%	1.60%	0.65	3.58%	3.58%	4.33%	0.82
10	237.6	4.34%	5.71%	2.01%	0.85	3.83%	4.91%	6.53%	0.91
11	341.5	3.71%	4.92%	1.67%	0.61	3.46%	3.85%	5.03%	0.85
12	373.4	3.32%	3.71%	1.37%	0.78	3.51%	3.31%	3.15%	0.77
13	482.9	3.05%	3.02%	1.24%	0.90	3.39%	3.03%	2.41%	0.80
14	482.2	3.12%	3.16%	1.21%	0.83	3.45%	3.29%	2.58%	0.83
15	449.7	3.60%	4.59%	1.51%	0.80	3.51%	3.70%	4.37%	0.87
16	418.1	3.73%	5.02%	1.62%	0.66	3.15%	3.92%	5.03%	0.83
17	392.7	3.55%	4.40%	1.83%	0.58	3.37%	3.73%	4.87%	0.81
46	486.2	3.04%	2.80%	1.45%	0.79	4.62%	3.19%	3.09%	0.77

		6−31G**				cc-pVDZ			
	V_{VDW}[b]	CED-VDW[c]	FFS-VDW[c]	FFS-CED[c]	shape[d]	CED-VDW[c]	FFS-VDW[c]	FFS-CED[c]	shape[d]
9	263.3	3.00%	4.07%	3.89%	0.74	4.43%	3.63%	4.84%	0.71
10	237.6	3.69%	5.49%	6.28%	0.84	5.70%	3.88%	7.73%	0.86
11	341.5	3.02%	4.41%	4.57%	0.76	4.43%	3.32%	5.58%	0.74
12	373.4	2.97%	3.54%	2.75%	0.77	4.15%	3.80%	3.61%	0.61
13	482.9	2.88%	3.16%	1.89%	0.64	3.90%	3.60%	2.52%	0.58
14	482.2	2.88%	3.43%	2.19%	0.74	3.96%	3.93%	2.89%	0.61
15	449.7	2.99%	4.12%	3.88%	0.75	4.39%	3.80%	4.84%	0.71
16	418.1	2.78%	4.61%	4.66%	0.62	4.14%	3.19%	5.68%	0.68
17	392.7	3.18%	4.18%	4.87%	0.65	4.69%	3.00%	5.75%	0.82
46	486.2	5.36%	3.32%	3.89%	0.64	6.70%	4.13%	4.43%	0.61

[a] CED − calculated electron density, FFS − fuzzy fused-sphere, VDW − van der Waals. [b] V_{VDW} − van der Waals surface volume in $bohr^3$/molecule. [c] Symmetric volume difference of the two specified surfaces expressed as a percentage of V_{VDW}. [d] Shape group method similarity between CED and FFS.

van der Waals surfaces in most cases. However, in cases where this increased similarity would be seen it needs to be remembered that this comes about as a result of a complementary solvent radius choice and not because the molecular surface model is any more adept at realistically representing electron density in bonding regions of the solvated molecule.

The shape group method similarity measure between the fuzzy fused-sphere and calculated electron density representations shows how the two representations would differ if the isosurface bounds were changed, like in a case where different van der Waals radii are used, leading to changes in volume. Effectively, as long as the calculated electron density can be thought of as the slightly distorted addition of atomic representations, the shape similarity between it and the fuzzy fused-sphere representation should be high, while low shape similarity values indicate large distortions of the calculated electron density from the surface created by adding atomic representations. For the HF/STO-3G sigma-bonded molecules, the shape similarity values are high, indicating the calculated electron density is much like a slightly distorted fuzzy fused-sphere representation.

As basis set size is increased, the calculated electron density is based on a larger number of molecular orbitals, and so the bonding and more electron-diffuse regions of molecules are better defined. Because of this a slight increase is seen in the CED-VDW and FFS-VDW values for the basis sets 3−21G, 6−31G**, and cc-pVDZ as compared to the STO-3G values for the same molecules. However, the FFS-CED values are still quite small, indicating high similarity between the fuzzy fused-sphere and calculated electron density representations. Overall, because sigma bonding can be described as cylindrical in nature, the overlap of two fuzzy spheres will model a σ bond well both in terms of the cylindrical electron distribution within the bond as well as in terms of the decrease in electron density as the perpendicular distance from the axis of the cylinder is increased.

The shape similarity numbers tell much the same story as the basis set size is increased from STO-3G to 3−21G to 6−31G**. Generally, small decreases in the similarity for all the sigma-bonded molecules are seen as the basis set size is increased, indicating that the calculated electron density is quite similar to added atomic representations throughout a large range of electron density isosurface values. Use of different sets of van der Waals radii should therefore not have a large impact on the comparability of the representations. This cannot be said, however, for the molecular electron densities calculated at the highest basis set level (cc-pVDZ). The small shape similarity values indicate that fuzzy fused-sphere (and by extension, discrete fused-sphere) surfaces are not adept at modeling the electron density through a range of isosurface values. Since the larger basis set should provide a more realistic representation of the electron density than a smaller basis set, this indicates fused-sphere models are not effectively modeling "real" sigma-bonding systems.

Table 2 shows data comparable to that of Table 1 for the set of molecules (**9**-**17**, **46**) with both sigma and pi bonding.

The data in Table 2 show larger relative symmetric volume difference values than seen in Table 1 for both the calculated electron density and fuzzy fused-sphere surfaces compared to the van der Waals surfaces as well as compared to each other. More specifically, as the basis set size is increased, there is a marked increase in the FFS-CED symmetric volume difference values, indicating the calculated electron

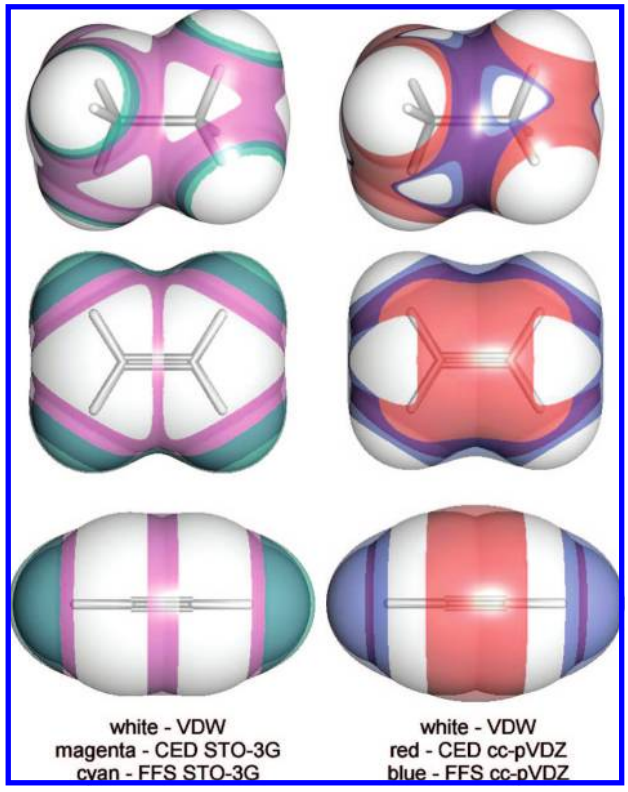

Figure 3. Equivolume van der Waals (VDW), fuzzy fused-sphere (FFS), and calculated electron density (CED) surfaces for ethane (**2**), ethene (**9**), and ethyne (**10**) at the HF/STO-3G and HF/cc-pVDZ levels of theory.

density can no longer be seen as slightly distorted added atomic representations. Pi bonding in the systems is the explanation for this observation. Pi bonding, unlike sigma bonding, is not cylindrical in nature, and so the overlap of spheres cannot represent it as well. This is confirmed as the smallest relative symmetric volume difference values in the table are seen for molecules **12**-**14**, where there are significant sigma-bonded regions of the molecules as well as pi-bonded regions. The values indicate these molecules fall in between those of Table 1 and the more significantly pi-bonded molecules of Table 2, showing that the sigma-bonded regions are somewhat well represented by the fused-sphere models but the pi bonding regions are not.

The notion that fused-sphere models are poor at representing pi bonding is further confirmed by the shape similarity values. In general, they are lower than those seen in Table 1, but more specifically, they are in many cases much smaller for molecules with double bonds. Ethene (**9**) is seen to have shape similarity numbers much smaller than those for ethane (**2**) for the basis sets STO-3G, 3−21G, and 6−31G**. The pi bonding of the double bond is directed in a plane that includes the axis of the σ bond and is characterized by fattening of the electron density between the atoms involved in the bonding. Since the cylindrical representation of bonding in fused-sphere models cannot include this directionality, this leads to lowered shape similarity to the calculated electron density. However, the ethyne (**10**) shape similarity numbers increase from those for ethene because the two perpendicular pi bonds do create a cylindrical electron density distribution. This, however, is a fortuitous

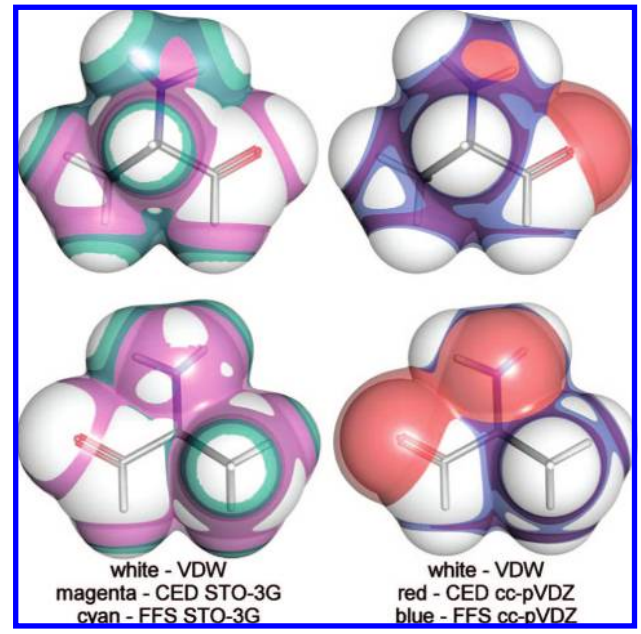

Figure 4. Front and back views of equivolume van der Waals (VDW), fuzzy fused-sphere (FFS), and calculated electron density (CED) surfaces for the alanyl group (**46**) at the HF/STO-3G and HF/cc-pVDZ levels of theory.

occurrence in the fused-sphere models rather than caused by adequate modeling of the electron density, as can be seen in Figure 3.

In Figure 3 equivolume van der Waals, fuzzy fused-sphere, and calculated electron density surfaces are shown for ethane, ethene, and ethyne at the HF/STO-3G and HF/cc-pVDZ levels. For ethane, the main difference between the van der Waals surface and the STO-3G calculated electron density surface is seen in the bonding regions of the molecule, as is to be expected. The FFS-VDW differences are most apparent in the carbon−hydrogen bonding regions, but for the most part, the two surfaces are not very different, as is seen in the symmetric volume difference data. In the HF/cc-pVDZ ethane representations, the calculated electron density shows many of the same differences from the van der Waals surface as for the smaller basis set, but the FFS-VDW comparison is much more complex.

The ethene molecule surfaces are most interesting. The STO-3G basis set, as a minimal basis, is not as effective at modeling pi bonding because of the small number of molecular orbitals, and so the calculated electron density does not show the characteristic pi-bond fattening except in the midpoint of the carbon−carbon bonding region. In the cc-pVDZ CED surface, the pi-bond fattening is quite evident, and so neither the VDW or FFS surface represents well the calculated electron density. The ethyne molecule surfaces also show these same features, but again, because of the cylindrical overlap of the two perpendicular pi bonds in the molecule, the VDW and FFS models more closely match the calculated electron density surfaces.

A molecule of special interest in the study is the hydrogen terminated representation of the alanyl group (**46**), which shows the basic features of amide linked amino acids as they are found in proteins, the most notable of which are the amino group and the carbonyl group. Table 2 contains the

Table 3. Similarity Comparisons for Selected Aromatic Group Molecules[a]

		STO-3G				3−21G			
	V_{VDW}[b]	CED-VDW[c]	FFS-VDW[c]	FFS-CED[c]	shape[d]	CED-VDW[c]	FFS-VDW[c]	FFS-CED[c]	shape[d]
18	557.8	3.21%	4.22%	1.34%	0.90	2.86%	3.32%	4.48%	0.87
19	668.5	3.10%	3.94%	1.31%	0.92	2.95%	3.20%	3.79%	0.85
20	599.6	3.22%	4.10%	1.61%	0.82	3.61%	3.30%	4.80%	0.81
21	602.7	3.05%	3.68%	1.16%	0.87	3.44%	3.09%	3.92%	0.87
27	710.2	3.14%	3.81%	1.51%	0.91	3.59%	3.21%	4.13%	0.84
28	711.5	3.14%	3.83%	1.52%	0.90	3.60%	3.22%	4.19%	0.83
29	710.1	3.14%	3.82%	1.52%	0.91	3.58%	3.19%	4.16%	0.87
39	610.2	3.11%	3.57%	1.07%	0.86	3.76%	3.02%	3.92%	0.85

		6−31G**				cc-pVDZ			
	V_{VDW}[b]	CED-VDW[c]	FFS-VDW[c]	FFS-CED[c]	shape[d]	CED-VDW[c]	FFS-VDW[c]	FFS-CED[c]	shape[d]
18	557.8	2.25%	3.77%	3.96%	0.88	3.71%	3.40%	4.98%	0.68
19	668.5	2.41%	3.57%	3.43%	0.83	3.77%	3.50%	4.45%	0.63
20	599.6	3.62%	3.93%	4.52%	0.82	5.07%	3.85%	5.34%	0.67
21	602.7	3.90%	3.46%	4.02%	0.81	5.19%	3.65%	4.86%	0.68
27	710.2	3.52%	3.72%	3.99%	0.85	4.89%	3.81%	4.79%	0.65
28	711.5	3.52%	3.72%	4.03%	0.86	4.93%	3.82%	4.90%	0.71
29	710.1	3.50%	3.72%	3.94%	0.87	4.90%	3.79%	4.75%	0.67
39	610.2	5.28%	3.70%	4.47%	0.79	6.52%	3.72%	5.11%	0.79

[a] CED − calculated electron density, FFS − fuzzy fused-sphere, VDW − van der Waals. [b] V_{VDW} − van der Waals surface volume in $bohr^3$/molecule. [c] Symmetric volume difference of the two specified surfaces expressed as a percentage of V_{VDW}. [d] Shape group method similarity between CED and FFS.

similarity data for the surfaces of this alanyl group, while Figure 4 shows front and back views of the van der Waals, the HF/STO-3G, and the HF/cc-pVDZ fuzzy fused-sphere and calculated electron density surfaces.

When considered in the group of molecules with both double bonds and significant sigma-bonding-only groups (**12**-**14**), the alanyl group FFS-VDW symmetric volume difference values occur at the low end of the range for STO-3G and then move toward the high end of the range as the basis set size is increased. In Figure 4 it can be seen that the main sources for this increase are the bonding regions of the hydrogen atoms, and the fuzzy-fused sphere overlaps between the groups that are bonded to the central carbon atom.

More importantly, the FFS-CED and the CED-VDW symmetric volume difference comparisons start in the same range of values as molecules **12**-**14** with the minimal basis set, but quickly fall outside of the range, becoming much larger (indicating lesser similarity) when the basis set size is increased. The shape similarity values confirm this trend, as lower similarity is seen as the basis set becomes larger, and the electron density is more realistically modeled.

Figure 4 shows that the STO-3G calculated electron density surface differs most in the bonding and group overlap regions, as has been seen before in ethane. For the cc-pVDZ CED, though, the largest differences are seen around the oxygen atom of the carbonyl group and the nitrogen atom of the amine group. If the electron density is considered in very simple terms these regions of the molecule include sigma-bonding, pi-bonding, and nonbonding electrons. With the double-bonded oxygen atom and its nonbonded electrons, the electron density tends to balloon outside of the fused-sphere representations anisotropically in various directions, while for the nitrogen atom this ballooning tends to occur in the region of the atom where the nonbonding electrons would be found. A sphere of fixed radius, regardless of how the radius is chosen, will not accurately model all three electron types at the same time.

The implication for fused-sphere modeling of polypeptides and proteins is clear. While the electron density sigma-bonding-only side chains of certain amino acids like glycine, alanine, valine, leucine, and isoleucine can somewhat be adequately modeled with fused-sphere representations, the backbone of the protein, with its carbonyl and amine groups, cannot be adequately modeled with fused-sphere representations. Additionally, the side chains of amino acids such as aspartic acid, glutamic acid, lysine, arginine, asparagine, and glutamine most likely face the same fused-sphere modeling difficulties as the backbone groups. Such a notion is supported by a study where parametrization of atomic radii to give agreement between van der Waals and solvent accessible surface-based Poisson−Boltzmann electrostatic free energy calculations show that for a single amino acid the atomic radii need to differ by 2−5% between the van der Waals and solvent accessible surface calculations, but for an approximately 200-residue protein this difference in atomic radii required to achieve agreement increases to over 20%.[8]

Table 3 gives the similarity comparisons for selected aromatic group (**18**-**45**) molecules. In comparison to ethene (**10**), the benzene molecule (**18**) CED-VDW symmetric volume difference values are markedly lower, indicating higher similarity. This higher similarity is also seen in the shape similarity values, with the exception for the HF/cc-pVDZ case, where little change is seen in the relatively poor similarity value. The high level of symmetry leads to this higher similarity, with the ring forming a toroidal distribution of electron density, which acts much like the cylindrical distribution of the electron density in both sigma and triple bonds. Figure 5 shows the surfaces at the HF/STO-3G and HF/cc-pVDZ levels for benzene. As seen before in ethene,

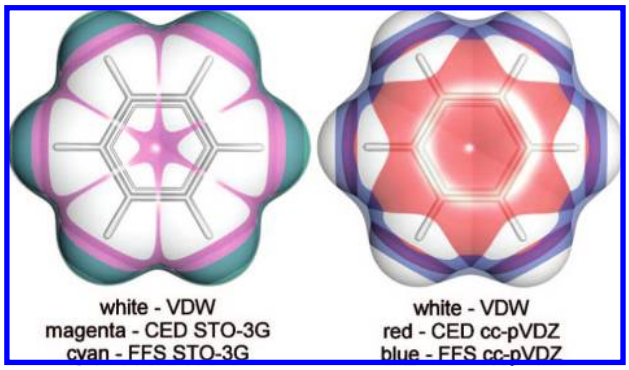

Figure 5. Equivolume van der Waals (VDW), fuzzy fused-sphere (FFS), and calculated electron density (CED) surfaces for benzene (**18**) at the HF/STO-3G and HF/cc-pVDZ levels of theory.

the minimal basis set does not model well the delocalization of the electron density above and below the plane of the ring, leading to the calculated electron density being much like a distorted fused-sphere representation where the most notable differences to the VDW surface are in the midpoints of the bonds. The larger basis set more accurately models this delocalization.

Molecules **21** and **39** in the table are highly conjugated ring compounds that are not aromatic. In terms of the symmetric volume difference values as the basis set size is increased, the trends in the changes in the values as compared to benzene are much like those of the alanyl molecule relative to molecules **12**-**14**, in that sigma-, pi-, and nonbonding electrons are being represented by a single fused-sphere radius, and so as the electron density is better modeled with larger basis sets, the differences become more marked.

Conclusion

Through the use of symmetric volume difference and the shape group method it has been shown that fused-sphere models and fuzzy fused-sphere models show significant differences to calculated electron densities of small molecules, even for a minimal basis set, where it would be expected the models should show reasonable similarity. Use of more complete basis sets only serve to highlight the increasing difference between fused-sphere models and calculated electron densities, especially as they relate to pi- and nonbonding regions of the molecules. Larger molecules, it can be concluded, will likely be even more poorly represented by fused-sphere or fuzzy fused-sphere models. As such, with advances in computing power, algorithm parallelization and linear scaling electron density methods, the use of calculated electron density models is recommended over fused-sphere models. In cases where fused-sphere based models are the only currently existing models in use for the calculation of a specific property, these results would also indicate that development and exploration of specific property models that are based on calculated electron density representations should be vigorously pursued.

Acknowledgment. We thank Drs. Thomas E. Exner and Jürgen Brickmann for the use of the MOLCAD II module[67−70] of the SYBYL molecular modeling package[71] in visualizing our results.

Supporting Information Available: Complete table of the similarity comparison data, including fuzzy fused-sphere and calculated electron density isocontour bound values, for all 46 molecules at six basis set levels. This material is available free of charge via the Internet at http://pubs.acs.org.

References

(1) Pauling, L. van der Waals and Nonbonded Radii of Atoms. In *The Nature of the Chemical Bond*, 3rd ed.; Cornell University Press: Ithaca, NY, 1960; pp 257−264.

(2) Lee, B.; Richards, F. M. *J. Mol. Biol.* **1971**, *55*, 379.

(3) Rush, T. S., III; Grant, J. A.; Mosyak, L.; Nicholls, A. *J. Med. Chem.* **2005**, *48*, 1489.

(4) Honig, B.; Nicholls, A. *Science* **1995**, *268*, 1144.

(5) Anisimov, V. M.; Lamoureux, G.; Vorobyov, I. V.; Huang, N.; Roux, B.; MacKerell, A. D., Jr. *J. Chem. Theory Comput.* **2005**, *1*, 153.

(6) Weiner, S. J.; Kollman, P. A.; Case, D. A.; Singh, U. C.; Ghio, C.; Alagona, G.; Profeta, S., Jr.; Weiner, P. *J. Am. Chem. Soc.* **1984**, *106*, 765.

(7) Zhu, J.; Shi, Y.; Liu, H. *J. Phys. Chem. B* **2002**, *106*, 4844.

(8) Tjong, H.; Zhou, H.-X. *J. Chem. Theory Comput.* **2008**, *4*, 507.

(9) Gerig, J. T. *J. Org. Chem.* **2002**, *68*, 5244.

(10) Lee, M. S.; Olson, M. A. *J. Phys. Chem. B* **2005**, *109*, 5223.

(11) Miertz, S.; Scrocco, E.; Tomasi, J. *Chem. Phys.* **1981**, *55*, 117.

(12) Harpaz, Y.; Gerstein, M.; Chothia, C. *Structure* **1994**, *2*, 641.

(13) Richards, F. M. *J. Mol. Biol.* **1974**, *82*, 1.

(14) Tsai, J.; Taylor, R.; Chothia, C.; Gerstein, M. *J. Mol. Biol.* **1999**, *290*, 253.

(15) Li, A.-J.; Nussinov, R. *Proteins* **1998**, *32*, 111.

(16) Gavezzotti, A. *J. Am. Chem. Soc.* **1983**, *105*, 5220.

(17) Finney, J. L. *J. Mol. Biol.* **1975**, *96*, 721.

(18) Gerstein, M.; Tsai, J.; Levitt, M. *J. Mol. Biol.* **1995**, *249*, 955.

(19) Pacios, L. F. *J. Chem. Inf. Comput. Sci.* **2001**, *41*, 1427.

(20) Connolly, M. L. *J. Am. Chem. Soc.* **1985**, *107*, 1118.

(21) Meyer, A. Y. *J. Comput. Chem.* **1988**, *9*, 18.

(22) Pacios, L. F. *J. Mol. Model.* **1995**, *1*, 46.

(23) Liang, J.; Edelsbrunner, H.; Fu, P.; Sudhakar, P. V.; Subramaniam, S. *Proteins* **1998**, *33*, 1.

(24) Liang, J.; Edelsbrunner, H.; Fu, P.; Sudhakar, P. V.; Subramaniam, S. *Proteins* **1998**, *33*, 18.

(25) Estrada, E. *J. Phys. Chem. A* **2002**, *106*, 9085.

(26) Hirano, S.; Toyota, S.; Kato, M.; Toda, F. *Chem. Commun.* **2005**, 3646.

(27) Li, X.-Z.; He, J.-H.; Liao, D.-Z. *Inorg. Chem. Commun.* **2005**, *8*, 939.

(28) Castro, M.; Nicolás-Vázquez, I.; Zavala, J. I.; Sánchez-Viesca, F.; Berros, M. *J. Chem. Theory Comput.* **2007**, *3*, 681.

(29) Bondi, A. *J. Phys. Chem.* **1964**, *68*, 441.

(30) Bondi, A. *J. Phys. Chem.* **1966**, *70*, 3006.

(31) O'Keeffe, M.; Brese, N. E. *J. Am. Chem. Soc.* **1991**, *113*, 3226.

(32) Rowland, R. S.; Taylor, R. *J. Phys. Chem.* **1996**, *100*, 7384.

(33) Tsai, J.; Voss, N.; Gerstein, M. *Bioinformatics* **2001**, *17*, 949.

(34) Böhm, H.-J.; Ahlrichs, R. *J. Chem. Phys.* **1982**, *77*, 2028.

(35) Badenhoop, J. K.; Weinhold, F. *J. Chem. Phys.* **1997**, *107*, 5422.

(36) Chauvin, R. *J. Phys. Chem.* **1992**, *96*, 9194.

(37) Deb, B. M.; Singh, R.; Sukumar, N. *J. Mol. Struct: THEOCHEM* **1992**, *259*, 121.

(38) Arteca, G. A.; Grant, N. D. *J. Comput.-Aided. Mol. Des.* **1999**, *13*, 315.

(39) Nag, S.; Banerjee, K.; Datta, D. *New J. Chem.* **2007**, *31*, 832.

(40) Row, T. N. G.; Parthasarathy, R. *J. Am. Chem. Soc.* **1981**, *103*, 477.

(41) Price, S. L.; Stone, A. J.; Lucas, J.; Rowland, R. S.; Thornley, A. E. *J. Am. Chem. Soc.* **1994**, *116*, 4910.

(42) Schiemenz, G. P. *Z. Naturforsch., B: Chem. Sci.* **2007**, *62b*, 235.

(43) Blinn, J. F. *ACM Trans. Graphics* **1982**, *1*, 235.

(44) Friedrichs, M.; Zhou, R.; Edinger, S. R.; Friesner, R. A. *J. Phys. Chem. B* **1999**, *103*, 3057.

(45) Grant, J. A.; Pickup, B. T. *J. Phys. Chem.* **1995**, *99*, 3503.

(46) Grant, J. A.; Gallardo, M. A.; Pickup, B. T. *J. Comput. Chem.* **1996**, *14*, 1653.

(47) Grant, J. A.; Pickup, B. T.; Nicholls, A. *J. Comput. Chem.* **2001**, *22*, 608.

(48) Pacios, L. F. *J. Phys. Chem.* **1991**, *95*, 10653.

(49) Pacios, L. F. *J. Phys. Chem.* **1992**, *96*, 7294.

(50) Pacios, L. F. *J. Phys. Chem.* **1994**, *98*, 3688.

(51) Pacios, L. F. *J. Comput. Chem.* **1995**, *16*, 133.

(52) Pacios, L. F. *J. Comput. Chem.* **2005**, *14*, 410.

(53) Hohenberg, P.; Kohn, W. *Phys. Rev.* **1964**, *136*, B864.

(54) Mezey, P. G. *Mol. Phys.* **1999**, *96*, 169.

(55) Mezey, P. G. Topological similarity of molecules and the consequences of the holographic electron density theorem, an extension of the Hohenberg-Kohn theorem. In *Fundamentals of Molecular Similarity*; Carbó-Dorca, R., Girones, X., Mezey, P. G. Eds.; Kluwer Academic/Plenum Publishers: New York, NY, 2001; pp 113−124.

(56) Goh, S. K.; St-Amant, A. *Chem. Phys. Lett.* **1997**, *264*, 9.

(57) Exner, T. E.; Mezey, P. G. *J. Comput. Chem.* **2003**, *24*, 1980.

(58) Skylaris, C.-K.; Haynes, P. D.; Mostofi, A. A.; Payne, M. C. *J. Chem. Phys.* **2005**, *122*, 084119.

(59) Skylaris, C.-K.; Haynes, P. D. *J. Chem. Phys.* **2007**, *127*, 164712.

(60) Mezey, P. G. *Shape in Chemistry: Introduction to Molecular Shape and Topology*; VCH Publishers: New York,1992.

(61) Mezey, P. G. *Int. J. Quant. Chem. Quant. Biol. Symp.* **1986**, *12*, 113.

(62) Mezey, P. G. *J. Comput. Chem.* **1987**, *8*, 462.

(63) Mezey, P. G. *Int. J. Quant. Chem. Quant. Biol. Symp* **1987**, *14*, 127.

(64) Mezey, P. G. *J. Math. Chem.* **1988**, *2*, 299.

(65) Mezey, P. G. *J. Math. Chem.* **1988**, *2*, 325.

(66) Walker, P. D.; Arteca, G. A.; Mezey, P. G. *J. Comput. Chem.* **1993**, *14*, 1172.

(67) Frisch, M. J.; Trucks, G. W.; Schlegel, H. B.; Scuseria, G. E.; Robb, M. A.; Cheeseman, J. R.; Montgomery, J. A., Jr.; Vreven, T.; Kudin, K. N.; Burant, J. C.; Millam, J. M.; Iyengar, S. S.; Tomasi, J.; Barone, V.; Mennucci, B.; Cossi, M.; Scalmani, G.; Rega, N.; Petersson, G. A.; Nakatsuji, H.; Hada, M.; Ehara, M.; Toyota, K.; Fukuda, R.; Hasegawa, J.; Ishida, M.; Nakajima, T.; Honda, Y.; Kitao,O.; Nakai, H.; Klene, M.; Li, X.; Knox, J. E.; Hratchian, H. P.; Cross, J. B.; Bakken, V.; Adamo, C.; Jaramillo, J.; Gomperts, R.; Stratmann, R. E.; Yazyev, O.; Austin, A. J.; Cammi, R.; Pomelli, C.; Ochterski, J. W.; Ayala, P. Y.; Morokuma, K.; Voth, G. A.; Salvador, P.; Dannenberg, J. J.; Zakrzewski, V. G.; Dapprich, S.; Daniels, A. D.; Strain, M. C.; Farkas, O.; Malick, D. K.; Rabuck, A. D.; Raghavachari, K.; Foresman, J. B.; Ortiz, J. V.; Cui, Q.; Baboul, A. G.; Clifford, S.; Cioslowski, J.; Stefanov, B. B.; Liu, G.; Liashenko, A.; Piskorz, P.; Komaromi, I.; Martin, R. L.; Fox, D. J.; Keith, T.; Al-Laham, M. A.; Peng, C. Y.; Nanayakkara, A.; Challacombe, M.; Gill, P. M. W.; Johnson, B.; Chen, W.; Wong, M. W.; Gonzalez, C.; Pople, J. A. *Gaussian 03 Revision B.05*; Gaussian, Inc.: Wallingford, CT, 2004.

(68) Waldherr-Teshner, M.; Goetze, T.; Heiden, W.; Knoblauch, M.; Volhardt, H.; Brickmann, J. MOLCAD - Computer Aided Visualization and Manipulation of Models in Molecular Science. At Second Eurographics Workshop on Visualization in Scientific Computing; Delft, Netherlands, 1991.

(69) Brickmann, J.; Keil, M.; Exner, T. E.; Marhöfer, R.; Moeckel, G. Molecular Models: Visualization. In *The Encyclopedia of Computational Chemistry*; Schleyer, P. v. R., Allinger, N. L., Clark, T., Gasteiger, J., Kollman, P. A., Schaefer, H. J., III, Schreiner, P. R. Eds.; John Wiley & Sons: Chichester, 1998.

(70) Brickmann, J.; Exner, T. E.; Keil, M.; Marhöfer, R. *J. Mol. Model.* **2000**, *6*, 328.

(71) *Sybyl 6.7*; Tripos, Inc.: 1699 South Hamley Road, St. Louis, MO 63144, 2000.

CT800268C